JOURNAL OF BACTERIOLOGY, July 2000, p. 3965–3971 Vol. 182, No. 14
0021-9193/00/$04.00+0
Copyright © 2000, American Society for Microbiology. All Rights Reserved.

Analysis of MinC Reveals Two Independent Domains Involved in Interaction with MinD and FtsZ

ZONGLIN HU AND JOE LUTKENHAUS*

Department of Microbiology, Molecular Genetics and Immunology, University of Kansas Medical Center, Kansas City, Kansas 66160

Received 2 February 2000/Accepted 21 April 2000

In *Escherichia coli* FtsZ assembles into a Z ring at midcell while assembly at polar sites is prevented by the *min* system. MinC, a component of this system, is an inhibitor of FtsZ assembly that is positioned within the cell by interaction with MinDE. In this study we found that MinC consists of two functional domains connected by a short linker. When fused to MalE the N-terminal domain is able to inhibit cell division and prevent FtsZ assembly in vitro. The C-terminal domain interacts with MinD, and expression in wild-type cells as a MalE fusion disrupts *min* function, resulting in a minicell phenotype. We also find that MinC is an oligomer, probably a dimer. Although the C-terminal domain is clearly sufficient for oligomerization, the N-terminal domain also promotes oligomerization. These results demonstrate that MinC consists of two independently functioning domains: an N-terminal domain capable of inhibiting FtsZ assembly and a C-terminal domain responsible for localization of MinC through interaction with MinD. The fusion of these two independent domains is required to achieve topological regulation of Z ring assembly.

In *Escherichia coli* the formation of two equal-sized daughter cells results from the formation of a Z ring, precisely at midcell, that directs septation (2). The Z ring is a cytoskeletal element that is formed by the self-assembly of FtsZ (6, 10, 11). In the absence of the *min* system, assembly of FtsZ is not limited to midcell but also occurs at the cell poles, resulting in polar Z rings and the formation of minicells (3, 18). This phenotype has led to the hypothesis that the cell poles contain potential division sites which are masked by the *min* system (4, 17).

The *min* system in *E. coli* consists of three genes, *minC*, *minD*, and *minE*, each of which is necessary for proper functioning of this system (4). Genetic and expression studies have revealed that *minC* encodes an inhibitor of division that is activated by MinD and topologically regulated by MinE (4, 5). Recent localization studies of functional Min proteins tagged with green fluorescent protein have provided some insight into this topological regulation and revealed a fascinating oscillation of MinC and MinD between the cell halves (7, 14, 15).

In most cells MinE is present in a ring at midcell (16), while MinD and MinC rapidly oscillate between the halves of the cell (7, 14, 15). This oscillation involves MinC and MinD localized at the membrane in one half the cell followed by a cytoplasmic phase and the appearance of MinC and MinD at the membrane in the other half of the cell. The localization of MinD and MinE is codependent and occurs independently of MinC (7, 14). The oscillation of MinC, however, is dependent upon MinD and MinE, with MinD interacting with MinC to bring it to the membrane (7, 15). The ability of MinD to concentrate MinC at the membrane is probably responsible for the 25- to 50-fold enhancement of MinC's inhibitory activity (8, 15).

Recent analysis of MinC indicated a mechanism for its inhibitory activity (8). MinC was found to interact directly with FtsZ to prevent polymerization, probably by destabilizing FtsZ filaments (8). Therefore, MinE and MinD can be viewed as a molecular oscillator that positions the MinC inhibitor at the membrane away from midcell where it is in position to destabilize FtsZ filaments before they mature into a Z ring. MinC is therefore a critical component of the division site selection system, as it must interact with both FtsZ and MinD. In this study we have found that MinC can be subdivided into two domains and each domain retains activity.

* Corresponding author. Mailing address: Department of Microbiology, Molecular Genetics and Immunology, University of Kansas Medical Center, Kansas City, KS 66160. Phone: (913) 588-7054. Fax: (913) 588-7295. E-mail: jlutkenh@kumc.edu.

MATERIALS AND METHODS

Strains and plasmids. The *E. coli* K-12 strains JS964 (MC1061 *malP*::*lacI*^{q} Δ*min*::*kan*) and JS219 (MC1061 *malP*::*lacI*^{q}, the isogenic *min*$^+$ parent of JS964) were used in this study (12). Plasmids pJC90 (*malE*), pZH101 (*malE-minC*) and pZH102 (*malE-minC19*) were constructed previously (7). In these plasmids the P_{BAD} promoter is located just upstream of *malE*. Additional in-frame fusions to *malE* were constructed by inserting appropriate restriction fragments into pJC90. An *Eco*RI-*Bam*HI fragment containing *minC* codons 1 to 115 (*minC*$^{1–115}$) was obtained from pJC22-5 (AD-MinC$^{1–115}$ [see below]) and inserted into pJC90 to give pZH111 (*malE-minC1*$^{1–115}$). An *Eco*RI-*Sal*I fragment was obtained from plasmid pJC22-7 (AD-MinC$^{116–231}$ [see below]) and inserted into pJC90 to give pZH112 (*malE-minC*$^{116–231}$). Plasmids utilized in the yeast two-hybrid assay were as follows: pJC41 (AD-MinD), pJC41-2 (BD-MinD), pJC22 (BD-MinC), pJC22-1 (AD-MinC), pJC22-2 (BD-MinC19), and pJC22-3 (AD-MinC19); the parental vectors pGAD424 (AD) and pGBT9 (BD) have been described previously (7). Additional plasmids constructed for the present study included pJC22-4 (BD-MinC$^{1–115}$), pJC22-5 (AD-MinC$^{1–115}$), pJC22-6 (BD-MinC$^{116–231}$), and pJC22-7 (AD-MinC$^{116–231}$). These plasmids were constructed by inserting the appropriate PCR fragments at the polylinker sites of pGAD424 or pGBT9. For pJC22-4 (BD-MinC$^{1–115}$) and pJC22-5 (AD-MinC$^{1–115}$) the following primers (underlined sequence is the restriction site indicated in parentheses after the sequence) were used: 5′-TAGCAGGAATTCAGCAACACGCCAATCGAGCTTAAA-3′ (*Eco*RI) and 5′-TAGCATGGATCCTTATGGAGCCTGCGGTGTGGGAGCTG-3′ (*Bam*HI). For pJC22-6 (BD-MinC$^{116–231}$) and pJC22-7 (AD-MinC$^{116–231}$) the primers were 5′-TAGCATGAATTCGCGCAAAATACAACGCCGGTCACA-3′ (*Eco*RI) and 5′-TAGCATGTCGACTCAATTTAACGGTTGAACGGTC-3′ (*Sal*I). The template used with these primers was pJPB210 (*minCDE*). The PCR fragments obtained were digested with the appropriate restriction enzymes and cloned into pGAD424 and pGBT9. pZH103 contains *minD* downstream of the *aad* promoter in pGB2 (7). pMalc (New England Biolabs) is a pBR322 vector that contains *malE* fused to a segment of *lacZ* encoding the α peptide.

Protein purification and sedimentation assay of polymerization of FtsZ. MalE-MinC$^{1–115}$ and MalE-MinC$^{116–231}$ were purified using affinity chromatography as previously described for MalE, MalE-MinC, and MalE-MinC19 (8). The purification of FtsZ and the sedimentation assay for FtsZ polymerization were described previously (8, 10). The amount of FtsZ in the pellet of the sedimentation assay for FtsZ polymerization was determined by solubilizing the pellet in 100 μl of sodium dodecyl sulfate (SDS) sample buffer and subjecting 20

Downloaded from jb.asm.org at Biblioteca do ITQB on December 15, 2008

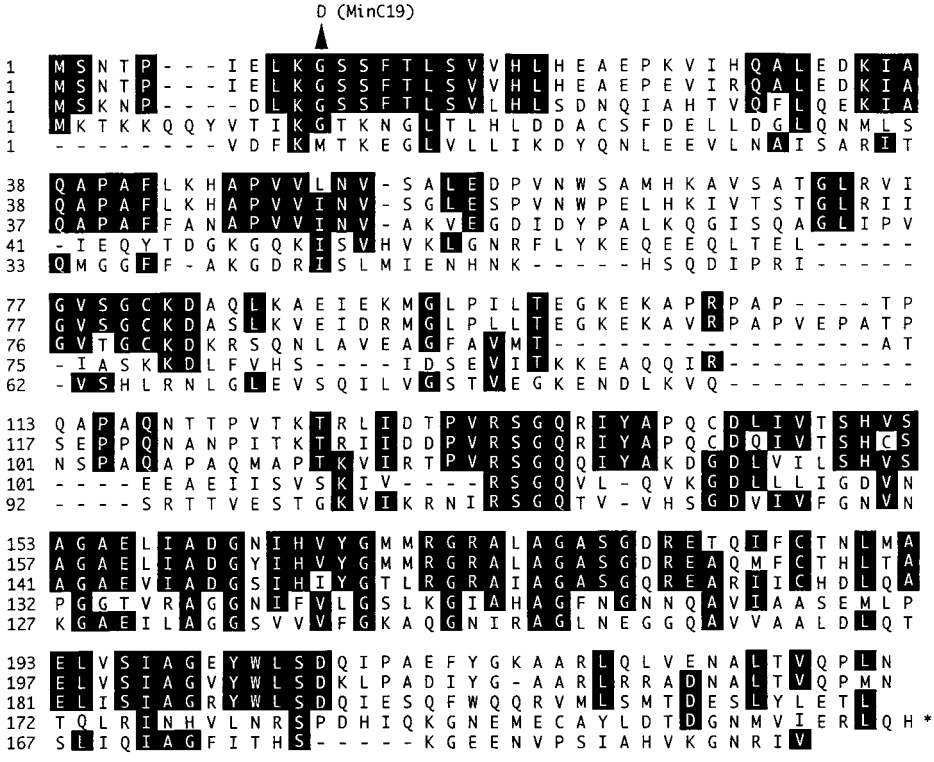

FIG. 1. Alignment of MinC sequences. The sequences of MinC from various bacteria were aligned using MegAlign (DNA Star) and the Clustal Method. Identical amino acids in three or more sequences are boxed. The MinC sequences (with GenBank accession numbers in parentheses) are, from the top, *E. coli* (AAB59061.1), *S. enterica* serovar Typhimurium, *V. cholerae*, *Bacillus subtilis* (AAA22400.1), and *T. maritima* (AAD36124.1). The asterisk indicates that the *B. subtilis* MinC is truncated and the last 15 residues are not shown.

μl to SDS-polyacrylamide gel electrophoresis (PAGE). After staining with Coomassie brilliant blue, the bands were quantitated with digital imaging equipment from Alpha Innotech (San Leandro, Calif.).

Yeast two-hybrid assay. To detect interactions the appropriate plasmids described above were transformed in various combinations into the reporter strain, SFY526 (1). The colonies obtained were analyzed for β-galactosidase production by both the colony lift assay and the quantitation assay as described in the CLONTECH manual.

Phenotypic analysis of the MalE fusions. Cultures were grown at 30°C in Luria-Bertani medium containing 100 μg of ampicillin per ml. The effect of MalE fusions on cell morphology was determined on plates and in liquid medium. In the liquid assays strains were grown overnight, subcultured, and grown to exponential phase for several hours. Arabinose was added to 0.005%, and samples were taken for photography 90 to 120 min later. Cells were photographed using a Nikon phase contrast microscope equipped with a charge-coupled device camera (Dage-MTI, Inc.). Images were captured using Flashpoint software (Integral Technologies, Inc.), and the figures were assembled using Adobe Photoshop.

Chromatography. Proteins were incubated at room temperature for 20 min in 275 μl of polymerization buffer (50 mM morpholineethanesulfonic acid–NaOH [pH 6.5], 50 mM KCl and 10 mM $MgCl_2$) before application to a fast-performance liquid chromatography Superose-6 column equilibrated with polymerization buffer also at room temperature. The eluate was monitored with a UV monitor, and either 24 1-ml or 60 0.4-ml fractions were collected. A 10-μl aliquot from each fraction was mixed with 10 μl of 2× SDS sample buffer and analyzed by SDS–10% PAGE.

MinC sequences. Some MinC sequences were obtained from the NCBI Microbial Unfinished Genomes Database. The MinC sequence for *Vibrio cholerae* was obtained from The Institute for Genomic Research website at http://www.tigr.org. The MinC from *Salmonella enterica* serovar Typhimurium was from the Washington University Genome Center.

RESULTS

Analysis of MinC sequences suggests two domains. MinC is present in a diverse group of bacteria, including gram-negative and gram-positive organisms as well as *Thermotoga maritima*, which lies near the root of the phylogenetic tree (13). Comparison of MinC sequences from several of these organisms suggests that MinC might be composed of two domains of approximately equal size connected by a linker (Fig. 1). The first domain consists of the N-terminal half of the protein and extends from residue 1 to two large hydrophobic residues followed by a threonine at positions 97 to 99 (the numbers are from the *E. coli* MinC). The N-terminal domain is not as conserved as the C-terminal domain but includes the region that contacts FtsZ as defined by the *minC19* mutation which alters residue 10 (12). This mutation reduces the affinity of MinC for FtsZ without affecting the interaction with MinD (8). The second domain is comprised of the C-terminal half of the protein and starts with a fairly conserved threonine at position 125. This domain contains a highly conserved region, residues 133 to 204, followed by a less-conserved carboxy tail. These two potential domains are connected by a linker of 14 to 29 amino acids in the sequences examined.

MinC is an oligomer. In our previous study on MinC function we generated a MalE-MinC fusion in order to facilitate purification (8). This fusion retained full biological function. Analysis of this fusion by size exclusion chromatography revealed that it was an oligomer (Fig. 2A). The calculated molecular weight of the fusion is 67,000 (67K); however, most of it eluted at a volume corresponding to a molecular weight of 170K, suggesting that the fusion is probably a dimer, possibly a trimer (Fig. 2C). In our previous study we also characterized the *minC19* mutation (8). This mutation, which changes Gly to Asp at amino acid 10, decreases the affinity of MinC for FtsZ but does not affect the interaction between MinC and MinD

Downloaded from jb.asm.org at Biblioteca do ITQB on December 15, 2008

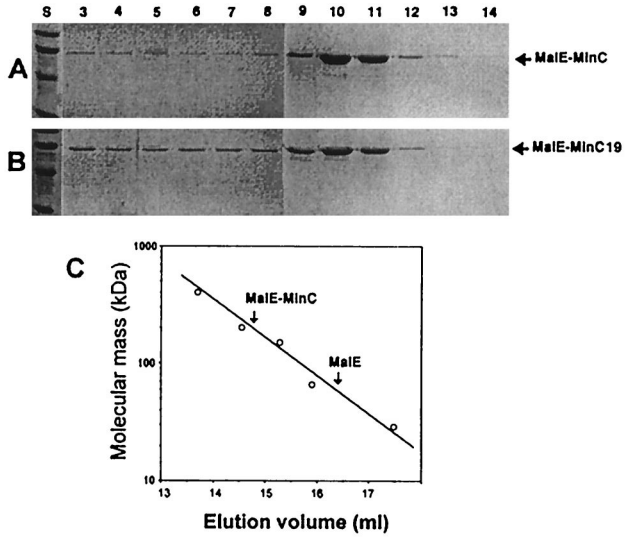

FIG. 2. Gel filtration chromatography of MalE-MinC and MalE-MinC19. Affinity-purified MalE-MinC was analyzed on a Superose-6 gel filtration column equilibrated with polymerization buffer. Fractions obtained from the elution were analyzed by SDS-PAGE (fraction number indicated at the top). (A and B) Lane S contains molecular weight markers (from the top, phosphorylase *b*, 97.4K; serum albumin, 66K; ovalbumin, 45K; and carbonic anhydrase, 29K). (A) A 1-ml sample of MalE-MinC (12.5 μM) was applied to the column; (B) a 1-ml sample of MalE-MinC19 (12 .5 μM) was applied to the column. (C) A standard curve for estimating the size of MalE-MinC was obtained by running the following molecular weight standards: apoferritin (400K), β-amylase (200K), alcohol dehydrogenase (150K), bovine serum albumin (66K), and carbonic anhydrase (29K).

(8). To determine if this mutation affects oligomerization of MinC, we analyzed the MalE-MinC19 fusion by size exclusion chromatography (Fig. 2B). This fusion eluted at the same position as the wild-type fusion, indicating that the *minC19* mutation did not affect MinC self-association. Although the majority of MalE-MinC and MalE-MinC19 eluted as a single peak, some of each fusion eluted between the peak and the void volume, indicating that there may be some aggregation.

The yeast two-hybrid system was also used to determine if MinC self-association could be detected. MinC was fused to both the binding and activation domains of the GAL4 protein. Introduction of the plasmids expressing these fusions into the yeast reporter strain SFY256 revealed a relatively strong interaction (Table 1). Replacing MinC with MinC19 did not affect the interaction. These results are consistent with the chromatography results, and we conclude that MinC self-associates to form at least a dimer and that this self-association is not noticeably affected by the *minC19* mutation.

TABLE 1. Analysis of MinC using the yeast two-hybrid system

Product fused to AD	Interaction with product fused to BD[a]		
	MinC	$MinC^{1–115}$	$MinC^{116–231}$
None	−	−	−
MinC	++	−	++
MinC19	++	−	−
$MinC^{1–115}$	−		−
$MinC^{116–231}$	++	−	++
MinD	+++	−	+++
FtsZ	−	−	−

[a] The strength of the interaction is based upon the color development using 5-bromo-4-chloro-3-indolyl-β-D-galactopyranoside: −, no color development in 24 h; +++, strong color development in <1 h; ++, color development between 1 and 3 h.

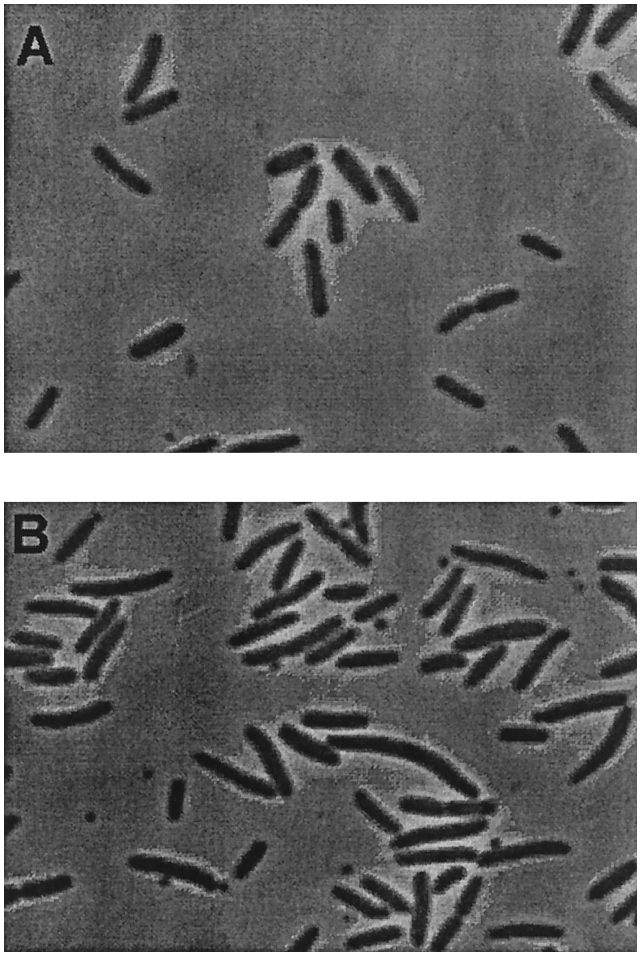

FIG. 3. Expression of the C-terminal domain of MinC induces minicell formation in wild-type cells. JS219 containing pJC90 (*malE*) (A) or pZH111 (*malE-minC*$^{116-231}$) (B) was diluted from an overnight culture and grown for several hours. Arabinose (0.005%) was added, and samples were taken for photography 2 h later.

Domain analysis using the yeast two-hybrid system. The above analysis along with previous results indicates that MinC binds at least three proteins, itself (this study), MinD and FtsZ (8, 9). To determine if the interacting surfaces could be assigned to one of the two putative domains of MinC we split MinC into two segments: positions 1 to 115 and positions 116 to 231, as suggested by the sequence analysis. Each segment was fused to the activation and binding domain of GAL4 and tested in the yeast two-hybrid system (Table 1). This analysis revealed that the C-terminal domain of MinC retained activity and interacted with itself and MinD. For both of these interactions the C-terminal domain appeared to be as active as the entire MinC protein, suggesting that the C-terminal domain of MinC functions independently of the N-terminal domain in these interactions. No additional information about the N-terminal domain was obtained in these studies as no binding was detected with other known possible partners (FtsZ, MinC, and MinD). We also tested for interaction between the N- and C-terminal domains of MinC but detected no interaction. We also confirmed our previous observation (9) that interaction

Downloaded from jb.asm.org at Biblioteca do ITQB on December 15, 2008

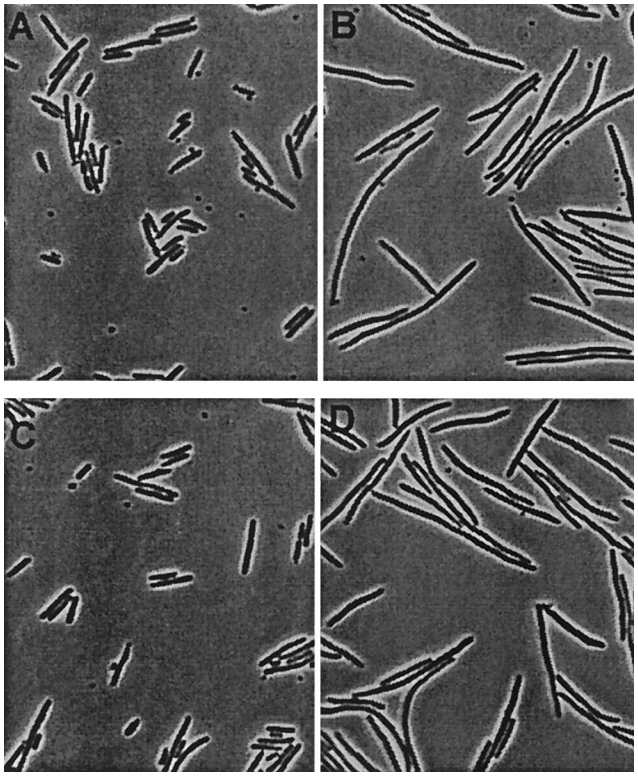

FIG. 4. Expression of the N-terminal domain of MinC induces filamentation. JS964 (Δ*min*) containing various MalE fusions was photographed 90 to 120 min after adding arabinose (0.005%) to exponentially growing cultures. The plasmids and fusions used were as follows: (A) pJC90 (*malE*), (B) pZH111 (*malE-minC*$^{1–115}$), (C) pZH112 (*malE-minC*$^{116–231}$), and (D) pZH101 (*malE-minC*).

between MinC and FtsZ, readily detected using physical methods (8), is not readily detected in this assay.

Functional analysis of the domains of MinC. The above analysis indicated that the interaction between MinC and MinD occurs through the carboxyl-terminal domain of MinC, which also appears responsible for the self-association of MinC. Although no interactions were observed with the N-terminal domain the location of the *minC19* mutation suggested that the N-terminal domain may interact with FtsZ. To further explore these possibilities we analyzed the effects of expression of these domains on cell morphology. To do this the two domains of MinC were fused to MalE and expressed in JS219 (*min*$^{+}$), and the phenotype was compared to that observed by induction of MalE and MalE-MinC. Under the conditions used, induction of MalE had no effect on cell morphology (Fig. 3A), whereas MalE-MinC induced filamentation (data not shown) as previously observed (8). Interestingly, expression of MalE-MinC$^{116–231}$ induced a minicell phenotype similar to that observed following deletion of the *min* locus (Fig. 3B). This phenotype includes minicells as well as cells longer than twice the newborn cell length, indicating the *min* system was inactive. A possible explanation for induction of this phenotype is competition between the C-terminal domain of MinC and full-length MinC for binding to MinD. Such interaction would be expected to disrupt the function of the *min* system because this truncated MinC is missing the domain of MinC required for inhibition of cell division and interaction with FtsZ (see below). In contrast to the effect of the C-terminal domain, expression of MalE-MinC$^{1–115}$ induced filamentation (data not shown). This was explored further using a Δ*min* strain.

The domains of MinC fused to MalE were expressed in JS964 (Δ*min*). In this strain the effects of the fusion cannot be ascribed to interactions with the other Min proteins. As shown previously (8) MalE-MinC, in the absence of MinD, inhibits division when expressed 25- to 50-fold over the physiological level (Fig. 4D). Expression of MalE and MalE-MinC$^{116–231}$ had no effect on cell morphology as a typical Min phenotype was observed (Fig. 4A and C, respectively). In contrast, expression of MalE-MinC$^{1–115}$ resulted in filamentation of the *min* mutant (Fig. 4B) just as it did in the wild-type strain. Comparison of the inhibitory effects of expression of this fusion to expression of MalE-MinC at various arabinose concentrations indicated that the N-terminal domain was as effective as the full-length MinC (data not shown). To support this conclusion the levels of the various fusions were examined following induction with 0.001% arabinose for 1 h. Gel analysis showed that the level of the C-terminal fusion was the same as the full-length MinC, whereas the N-terminal fusion was threefold higher (data not shown). This result indicates that the N-terminal fusion may be somewhat less active than the full-length MinC but demonstrates that the division-inhibitory ac-

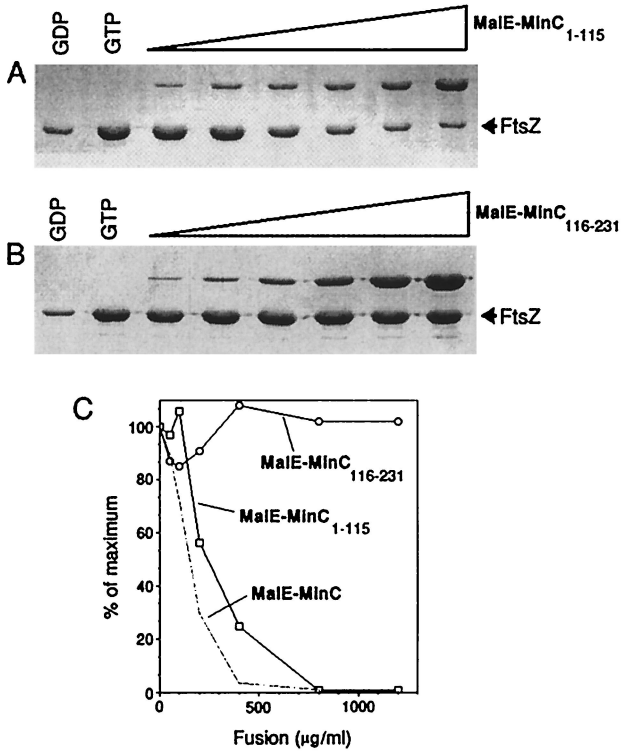

FIG. 5. The N-terminal domain of MinC is sufficient to prevent FtsZ polymerization. Affinity-purified MalE-MinC$^{1–115}$ and MalE-MinC$^{116–231}$ were tested for their effect on FtsZ polymerization utilizing a sedimentation assay. FtsZ at 200 μg/ml was incubated in polymerization buffer (50 mM morpholineethanesulfonic acid [pH 6.5], 50 mM KCl, 1 mM $MgCl_2$) with increasing concentrations of the MalE fusions. The reactions were initiated by the addition of GTP at 1 mM. After a 5-min incubation at room temperature the samples were centrifuged at 80K rpm for 15 min in a Beckman TLA 100.2 rotor. The pellets were resuspended in SDS sample buffer and analyzed by SDS-PAGE. (A and B) Lanes GDP contain a control with GDP added, and lanes GTP contain GTP but no fusion protein. The final concentration of fusion protein added (in micrograms per milliliter) was 50, 100, 200, 400, 800, and 1,200 in lanes 3 to 8, respectively. (C) The amount of FtsZ in the pellet was plotted as a percentage of the control lacking the fusion protein. The data for MalE-MinC was taken from reference 8.

Downloaded from jb.asm.org at Biblioteca do ITQB on December 15, 2008

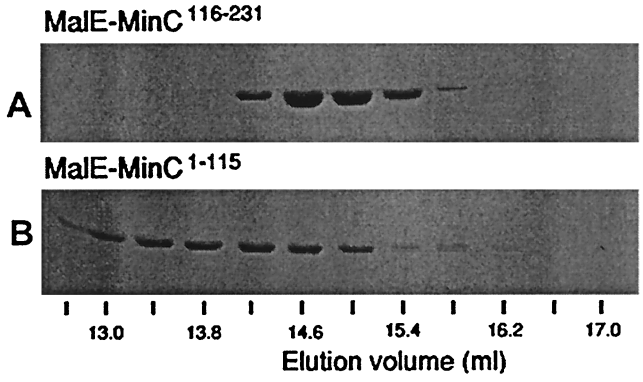

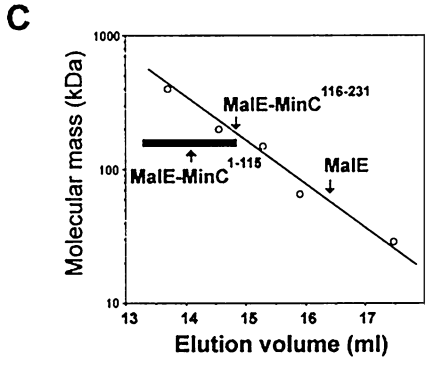

FIG. 6. The C-terminal and N-terminal domains of MinC promote oligomerization. MalE-MinC$^{1-115}$ and MalE-MinC$^{116-231}$ were analyzed by gel filtration chromatography as described in the legend to Fig. 2, except that smaller fractions were collected. (A and B) Fractions from the elution were analyzed by SDS-PAGE. (C) The same standard curve shown in Fig. 2 was used to estimate the size of the fusions.

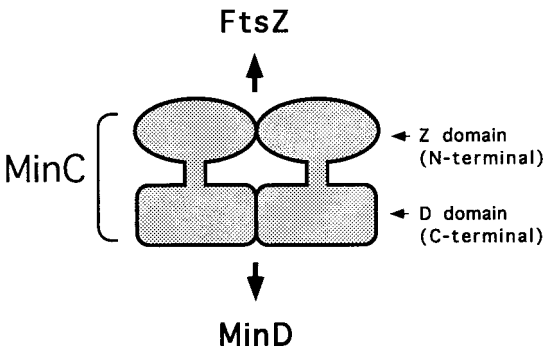

FIG. 7. Model of MinC. In this model MinC is depicted as a dimer although it is possible that it forms larger oligomers. The N-terminal domain (Z domain) interacts with FtsZ to prevent polymerization. The C-terminal domain (D domain) is responsible for interaction with MinD resulting in placement of MinC at the membrane. It is not clear if dimerization plays a role in these interactions. The C-terminal domain is clearly sufficient for dimerization, although in vitro results show that the N-terminal domain may also contribute to dimerization. The N-terminal domain also promotes the formation of oligomers larger than dimers. This activity is partially suppressed in the full-length MinC.

tivity of MinC resides within the N-terminal domain. Furthermore, the results clearly demonstrate that the N-terminal domain can inhibit division in the absence of the C-terminal domain.

Although MinC alone is able to inhibit division, it is a more effective inhibitor in the presence of MinD (5). Transformation of JS964 containing pZH101 (*malE-minC*) with a compatible plasmid (pZH103) expressing *minD* resulted in filamentous cells, even in the absence of arabinose (8). The presence of MinD did not enhance the inhibitory effect of MalE-MinC$^{1-115}$, as JS964 containing pZH111 (*malE-minC*$^{1-115}$) and pZH103 had a typical Min phenotype (data not shown). This result was expected since the yeast two-hybrid results demonstrated that MinD interacted with MinC through its C-terminal domain. Together these results demonstrate that the N-terminal domain of MinC has the ability to inhibit division but is unable to be activated by MinD.

The N-terminal domain of MinC is sufficient to inhibit FtsZ polymerization. We previously found that MinC prevents FtsZ polymerization as assayed by sedimentation and electron microscopy (8). To determine if the N-terminal subdomain of MinC retained this ability we purified MalE-MinC$^{1-115}$ and tested its activity in a sedimentation assay for FtsZ polymerization. As a control we used MalE-MinC$^{116-231}$. The results of this assay (Fig. 5A) demonstrated that MalE-MinC$^{1-115}$ is an effective inhibitor of FtsZ polymerization. In contrast, MalE-MinC$^{116-231}$ had no inhibitory activity (Fig. 5B). As noted previously (8), the pellets were not washed in this assay before they were analyzed by SDS-PAGE, so they are contaminated by the MalE fusions. Comparison of the activity of MalE-MinC$^{1-115}$ to the full-length MinC reveals that the N-terminal subdomain is about 50% as active as the full-length MinC (Fig. 5C). The fact that the N-terminal domain is almost as active as the full-length MinC (in the absence of MinD) in both inhibition of cell division and preventing FtsZ polymerization suggests that oligomerization of MinC is not important for these activities. However, this may not be the case, as the N-terminal domain also oligomerizes (see below). The main difference between MinC and MinC$^{1-115}$ is that the latter cannot be activated by MinD.

Self-association of MinC. Gel chromatography demonstrated that MalE-MinC was an oligomer (Fig. 2). The yeast two-hybrid studies also demonstrated that MinC self-associates and indicated that self-association occurred through the C-terminal domain (Table 1). To test this directly MalE-MinC$^{1-115}$ and MalE-MinC$^{116-231}$ were analyzed by size-exclusion chromatography along with MalE-α as a control (note that MalE-α is a fusion of MalE to the part of *lacZ* corresponding to the α peptide which is present in the pMalc vector). MalE-α eluted in a single peak, and the elution volume indicated a molecular weight of 60K, slightly larger than the calculated molecular weight of 50K, but consistent with it being a monomer (Fig. 6). MalE-MinC$^{116-231}$ also eluted as a single peak; however, the elution volume indicated a molecular weight of 160K (the calculated molecular weight of a monomer is 55K). This suggests that, like MalE-MinC, MalE-MinC$^{116-231}$ is probably also a dimer. Noticeably absent from the MalE-MinC$^{116-231}$ elution profile was the trail extending from the peak to the void volume that was observed with both MalE-MinC and MalE-MinC19 (Fig. 2).

In contrast to the results with the C-terminal domain, MalE-MinC$^{1-115}$ (monomer molecular weight of 54K) eluted over a larger volume, corresponding to a molecular weight range of 160K to >300K. These results indicate that both the C-terminal and N-terminal domains of MinC can promote oligomerization. A diagram indicating the domain structure of MinC is shown in Fig. 7.

Downloaded from jb.asm.org at Biblioteca do ITQB on December 15, 2008

DISCUSSION

Rod-shaped cells like *E. coli* utilize the *min* system to prevent the formation of polar Z rings, thereby ensuring that a Z ring only forms at midcell. This activity of the *min* system is achieved by topological regulation of MinC, an inhibitor of FtsZ polymerization (8). This inhibitor oscillates between the two halves of the cell through interaction with the MinDE oscillator (7, 15). For MinC to function it must contact both FtsZ and MinD. In this study we have found that these two interactions of MinC can be assigned to two functionally separable domains: an N-terminal domain which interacts with FtsZ and a C-terminal domain which interacts with MinD. Interestingly, each of these domains is also capable of mediating oligomerization.

The sequence alignments of MinCs from several bacteria (Fig. 1) raised the possibility that MinC might be composed of two domains connected by a short linker. Our present studies, in which the two domains were fused to various proteins for functional and biochemical analysis, confirm this possibility. Therefore, we designate the N-terminal domain as the Z domain, since it interacts with FtsZ, and the C-terminal domain as the D domain, since it interacts with MinD.

Our results also demonstrate that MinC is an oligomer. Both the yeast two-hybrid studies and gel chromatography supported this conclusion. The gel chromatography results indicated that MalE-MinC was a dimer or possibly a trimer. We think it likely that it is a dimer and the slightly larger size estimated from the gel chromatography may be due to the shape associated with a fusion of two globular domains. The yeast two-hybrid studies also indicated that the oligomerization activity could be assigned to the D domain of MinC, and this was confirmed by fusing the D domain to MalE and demonstrating that the fusion oligomerizes. Both of these assays indicate that this oligomerization is comparable to that observed with the intact MinC. Although the yeast two-hybrid study did not indicate any self-interaction of the Z domain, surprisingly, the fusion of this domain to MalE also resulted in oligomerization. It is possible that this domain is degraded or not folded properly in yeast. The broad elution profile of MalE-MinC$^{1-115}$ indicated that this domain promoted oligomers larger than the D domain and more than full-length MinC. This raises the possibility that this activity may be partially masked in the full-length MinC and exposed in the truncated MinC. It is also possible that the N-terminal domain is responsible for the larger aggregates observed during chromatography of MalE-MinC and MalE-MinC19. It is not clear what role the dimerization of MinC plays in its function.

To analyze the cell division-inhibitory activity of MinC we took advantage of the fact that overexpression of MinC, even in the absence of MinD, blocks cell division (5, 8). When the two domains of MinC were tested for inhibitory activity after fusion to MalE, only the Z domain was inhibitory. This domain of MinC is almost as active as the full-length MalE-MinC fusion (within two- to threefold) in both inhibiting FtsZ polymerization and inhibiting cell division. This implies that it interacts similarly with FtsZ. The assignment of FtsZ interaction to the N-terminal domain in this study is consistent with the location of the *minC19* mutation. This mutation, which results in a Gly10-Asp substitution, lowers the affinity of MinC for FtsZ and its ability to interfere with FtsZ polymerization. We have also altered additional residues on either side of amino acid 10, and several of them lead to mutant proteins with reduced activity similar to that of MinC19 (Qu and Lutkenhaus, unpublished data).

Although MinC is the inhibitor of FtsZ assembly, and therefore cell division, MinD is necessary for efficient inhibition. This stimulatory effect of MinD is estimated to be 25- to 50-fold (5) and is probably due to the MinD-dependent concentration of MinC at the membrane (7, 15). This recruitment is likely to involve a direct interaction between MinC and MinD, as we previously found that these proteins interact in the yeast two-hybrid system (9). In this study we have also used this test system to demonstrate that the C-terminal domain, in addition to promoting oligomerization, is also responsible for interaction with MinD. This conclusion is also supported by the observed phenotypic effects of expressing the separate domains. The N-terminal domain inhibited division when overexpressed, but this activity was not enhanced by MinD. Also, expression of the C-terminal domain in wild-type cells caused a minicell phenotype. A competition of the D domain with full-length MinC would be expected to upset the topological regulation of division. As the concentration of the D domain rises in the cell, the MinDE oscillator would be shuffling a truncated MinC that is unable to interact with FtsZ and prevent formation of polar Z rings.

The results of the present study demonstrate the modular composition of MinC. It contains different domains that are responsible for the interaction with FtsZ and MinD. The C-terminal domain of MinC is responsible, through its interaction with MinD, for localization to the membrane and oscillation between the halves of the cell. Thus, this domain is necessary to achieve the proper topological regulation. The N-terminal domain of MinC, through its interaction with FtsZ, is responsible for its ability to inhibit division by preventing FtsZ polymerization. Thus, our results show that topological regulation of division is achieved through the fusion of a domain responsible for its localization within the cell with a domain responsible for inhibiting FtsZ polymerization.

ACKNOWLEDGMENTS

This work was supported by grant GM29764 from the National Institutes of Health.

We thank the Genome Sequencing Center, Washington University, St. Louis, Mo., and the Institute for Genomic Research for releasing sequence information before publication.

REFERENCES

1. **Bartel, P. L., C.-T. Chien, R. Sternglanz, and S. Fields.** 1993. Elimination of false positives that arise in using the two-hybrid system. BioTechniques **14:**920–924.
2. **Bi, E., and J. Lutkenhaus.** 1991. FtsZ ring structure associated with division in *Escherichia coli*. Nature **354:**161–164.
3. **Bi, E., and J. Lutkenhaus.** 1993. Cell division inhibitors SulA and MinCD prevent formation of the FtsZ ring. J. Bacteriol. **175:**1118–1125.
4. **de Boer, P. A. J., R. E. Crossley, and L. I. Rothfield.** 1989. A division inhibitor and a topological specificity factor coded for by the minicell locus determine the proper placement of the division site in *Escherichia coli*. Cell **56:**641–649.
5. **de Boer, P. A. J., R. E. Crossley, and L. I. Rothfield.** 1992. Roles of MinC and MinD in the site-specific septation block mediated by the MinCDE system of *Escherichia coli*. J. Bacteriol. **174:**63–70.
6. **Erickson, H. P., D. W. Taylor, K. A. Taylor, and D. Bramhill.** 1996. Bacterial cell division protein FtsZ assembles into protofilament sheet and minirings, structural homologs of tubulin polymers. Proc. Natl. Acad. Sci. USA **93:**519–523.
7. **Hu, Z., and J. Lutkenhaus.** 1999. Topological regulation of cell division in E. coli involves rapid pole to pole oscillation of the division inhibitor MinC under the control of MinD and MinE. Mol. Microbiol. **34:**82–90.
8. **Hu, Z., A. Mukherjee, S. Pichoff, and J. Lutkenhaus.** 1999. The MinC component of the division site selection system in *E. coli* interacts with FtsZ and prevents polymerization. Proc. Natl. Acad. Sci. USA **96:**14819–14824.
9. **Huang, J., C. Cao, and J. Lutkenhaus.** 1996. Interaction between FtsZ and inhibitors of cell division. J. Bacteriol. **178:**5080–5085.
10. **Mukherjee, A., and J. Lutkenhaus.** 1994. Guanine nucleotide-dependent assembly of FtsZ into filaments. J. Bacteriol. **176:**2754–2758.
11. **Mukherjee, A., and J. Lutkenhaus.** 1998. Dynamic assembly of FtsZ regulated by GTP hydrolysis. EMBO J. **17:**462–469.

Downloaded from jb.asm.org at Biblioteca do ITQB on December 15, 2008

12. **Mulder, E., C. L. Woldringh, F. Tetart, and J.-P. Bouche.** 1992. New *minC* mutations suggest different interactions of the same region of division inhibitor MinC with proteins specific for *minD* and *dicB* coinhibition pathways. J. Bacteriol. **174:**35–39.
13. **Nelson, K. E., R. A. Clayton, S. R. Gill, M. L. Gwinn, R. J. Dodson, D. H. Haft, E. K. Hickey, J. D. Peterson, W. C. Nelson, K. A. Ketchum, L. McDonald, T. R. Utterback, J. A. Malek, K. D. Linher, M. M. Garrett, A. M. Stewart, M. D. Cotton, M. S. Pratt, C. A. Phillips, D. Richardson, J. Heidelberg, G. G. Sutton, R. D. Fleischmann, O. White, S. L. Salzberg, H. O. Smith, J. C. Venter, and C. M. Fraser.** 1999. Evidence for lateral gene transfer between Archaea and Bacteria from genome sequence of *Thermotoga maritima*. Nature **399:**323–329.
14. **Raskin, D. M., and P. A. de Boer.** 1999. Rapid pole-to-pole oscillation of a protein required for directing division to the middle of *Escherichia coli*. Proc. Natl. Acad. Sci. USA **96:**4971–4976.
15. **Raskin, D. M., and P. A. de Boer.** 1999. MinDE-dependent pole-to-pole oscillation of division inhibitor MinC in *Escherichia coli*. J. Bacteriol. **181:** 6419–6424.
16. **Raskin, D. M., and P. A. J. de Boer.** 1997. The MinE ring: an FtsZ-independent cell structure required for selection of the correct division site in *E. coli*. Cell **91:**685–694.
17. **Teather, R. M., J. F. Collins, and W. D. Donachie.** 1974. Quantal behavior of a diffusible factor which initiates septum formation at potential division sites in *E. coli*. J. Bacteriol. **118:**407–413.
18. **Yu, X.-C., and W. Margolin.** 1999. FtsZ ring clusters in min and partition mutants: role of both the Min system and the nucleoid in regulating FtsZ ring localization. Mol. Microbiol. **32:**315–326.

Downloaded from jb.asm.org at Biblioteca do ITQB on December 15, 2008